

## A theoretical study of the magneto-optical Kerr effect in FeX (X=Co,Ni,Pd,Pt)

This article has been downloaded from IOPscience. Please scroll down to see the full text article.

1994 J. Phys.: Condens. Matter 6 285

(<http://iopscience.iop.org/0953-8984/6/1/028>)

View [the table of contents for this issue](#), or go to the [journal homepage](#) for more

Download details:

IP Address: 171.66.16.159

The article was downloaded on 12/05/2010 at 14:32

Please note that [terms and conditions apply](#).

# A theoretical study of the magneto-optical Kerr effect in FeX (X=Co, Ni, Pd, Pt)

I Osterloh, P M Oppeneer†, J Sticht† and J Kübler

Institut für Festkörperphysik, Technische Hochschule Darmstadt, D-64283 Darmstadt, Federal Republic of Germany

Received 16 August 1993, in final form 28 October 1993

**Abstract.** The magneto-optical (MO) Kerr effect of FeX compounds with X=Co, Ni, Pd, Pt is studied theoretically using self-consistent band structure calculations. The MO spectra so determined agree with experimental Kerr spectra in overall shape but not in magnitude, the latter being slightly underestimated for FeCo and overestimated for FePd and FePt. The trend in the spectra for FeNi, FePd and FePt is explored and by investigating the effect of different crystal structures for FeCo and FePd we demonstrate that the Kerr spectrum depends sensitively on the local atomic environment of the Fe and Pd or Co atoms. Our calculations suggest that the computed spectra are those of highly ideal samples, which only approximately possess the atomic characteristics of the surfaces and bulk of real polycrystalline samples.

## 1. Introduction

Recent computational developments in band structure methods have made it possible to make reliable predictions of the magneto-optical (MO) Kerr spectrum on a first-principles basis [1–6]. The MO Kerr effect is found when polarized light is reflected from the surface of a magnetic material. The rotation angle of the polarization direction of the reflected light with respect to the incoming polarization is the so-called Kerr angle. This angle depends primarily on the photon energy, hence the term ‘Kerr spectrum’, but also on the geometry of the set-up, surface and magnetization direction. Here we consider only the polar Kerr effect for which both the magnetization and the incident photon wave vector are perpendicular to the surface.

The recent computational developments have led to an improved understanding of the physics underlying the MO Kerr effect. For instance, although it has been clear for quite some time that the Kerr effect is due to the interplay of spin-orbit coupling and exchange splitting (or magnetization) (see, e.g., the surveys [7] and [8]), it was not possible to understand in detail the origin of the spectral features of the MO spectra. Now, however, an understanding of the gross spectral features is gradually emerging [4–6]. In addition, through these computational developments the computer-aided search for MO materials suitable for optical data storage devices has been and will be further stimulated by searching for guidelines to tailor these materials [5, 9]. In some cases theoretical investigations have already triggered preparation and experimental research [10, 11].

† Present address: Max-Planck Arbeitsgruppe ‘Theorie komplexer und korrelierter Elektronensysteme’, Technische Universität, Abteilung Physik, Mommsenstrasse 13, D-01069 Dresden, Federal Republic of Germany.

‡ Present address: Biosym Technologies Incorporated, 9685 Scranton Road, San Diego, CA 92121, USA.

From a technological point of view, FePd and FePt compounds have interesting MO spectra, possessing peaks at 4–4.5 eV in the UV spectral range [12–14]. It is this peak at about 4 eV that these materials have in common with other prospective MO recording materials such as, for instance, CoPd and CoPt alloys [12, 15] as well as multilayers [16]. The Co atoms, however, induce a stronger magnetic anisotropy and, hence, the Co compounds are technologically more favourable for MO recording than the Fe compounds. A feature common for both types of compound is the pronounced influence of Pd and Pt on the electronic structure and, consequently, on the Kerr spectra.

The alloy FeCo has recently received experimental [17] and theoretical [18, 19] attention, but these early calculations must be called preliminary. The optical conductivity of Fe<sub>3</sub>TM (TM = Rh, Pd and Pt) alloys was studied theoretically by Ebert and Akai [2] and recently another theoretical study of FePt<sub>3</sub> was carried out by Halilov and Feder [6] with success.

This paper is organized as follows. After a brief description of the computational method in section 2 we begin in section 3 with FeCo for which our results demonstrate that we can predict the Kerr spectrum satisfactorily. Subsequently the trend in the spectra of FeNi, FePd and FePt is exposed and explained. When possible we compare with experimental data. For the cases of FeCo and FePd we investigate the effect of different atomic environments by performing calculations for different crystal structures. In section 4 we discuss our results and put them into a wider perspective.

## 2. Computational details

Our computational method was previously described in detail [4]. Here we merely mention that we use a linearized band structure method (ASW [20]), which is similar to the LMTO method [21]. The spin-orbit interaction is taken into account by performing a second variation on the spin-orbit Hamiltonian which is carried to self-consistency. The necessary atomic sphere radii were obtained by minimizing the total energy for a fixed cell volume; this always resulted in neutral atomic spheres. From the self-consistent band structure we then calculate the complex optical conductivity tensor by carrying out Brillouin zone integrations over all allowed interband transitions [4]. In these integrations, a phenomenological lifetime parameter is included in order to describe approximately finite lifetime effects in the self-energy. In terms of the conductivity tensor the polar Kerr angle is given by

$$\phi_K = \text{Re} \left\{ \frac{-\sigma_{xy}}{\sigma_{xx}} \left( \sqrt{1 + \frac{4\pi}{\omega} i\sigma_{xx}} \right)^{-1} \right\}. \quad (1)$$

The intraband contribution to the conductivity tensor is not considered in this paper. Both the influence of the intraband conductivity and the lifetime parameter have been explored previously [4]. We add, however, that we use different lifetime parameters for different compounds. This shortcoming of our otherwise *ab initio* theory is justified in the following section. With respect to our earlier calculations for FeCo [17, 18] we mention that we have now calculated the spectra with a newer version of our program [22], in which the energy bands are approximated quadratically within one tetrahedron, instead of linearly as was done previously. This allows us to compute the interband MO spectra accurately in the limit of zero photon energy, which carries over to the Kerr rotation at higher photon energies, which then also becomes slightly modified.

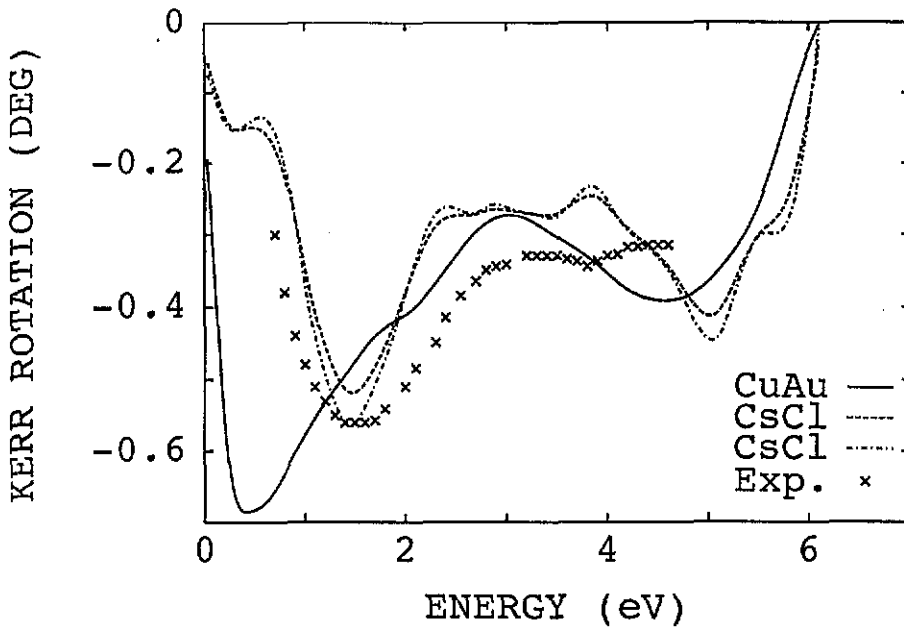


Figure 1. Experimental and calculated Kerr spectrum of FeCo. The experimental results are those of Weller *et al* [17]. The solid curve is computed using the CuAu structure, the dashed and dashed-dotted curves are obtained using the CsCl structure with the experimental atomic volumes. The lifetime parameter is 0.20 eV for the dashed-dotted curve and 0.27 eV for the dashed curve.

### 3. Results

#### 3.1. FeCo

In figure 1 we show the computed Kerr spectrum for FeCo and compare with the experimental results of Weller *et al* [17]. Although the stable form of FeCo has the CsCl structure with a lattice constant of  $a = 2.8492 \text{ \AA}$  [23] (which we used for our calculations) we repeated the calculations using for FeCo the CuAu structure with the same atomic volume as the CsCl structure, in order to show the influence of the crystallographic phase. The calculated total energy unambiguously favours the CsCl structure. For this structure the Kerr spectrum was calculated using two lifetime parameters, 0.27 eV and 0.20 eV. Figure 1 demonstrates how with decreasing lifetime parameters the calculated results partially approach the experimental values, the smaller lifetime parameter being a lower limit since small peaks not present in the experimental spectrum appear. The Kerr spectrum calculated using the CuAu structure (with a lifetime parameter of 0.4 eV) appears to be inferior. Regarding the peak at 0.5 eV, however, one should remember that the results shown do not include the intraband Drude conductivity. In fact, one can experiment with the Drude term trying different parameters; one finds that it is mostly the spectrum below 1 eV that is affected strongly by the Drude term and, indeed, shifting the peak at about 0.5 eV is not difficult. Turning to the CsCl structure, we note that the experimental peak at 1.5 eV is reproduced nicely by our calculations. For the remaining discrepancies, i.e. the height of the plateau at 3–4 eV and the theoretical peak at 4–5 eV, we can offer

three explanations. First, our calculated magnetic moments (spin and orbital contributions added) are somewhat smaller than the experimental values [24], our average moment per atom being  $2.27\mu_B$  versus  $2.40\mu_B$  experimentally. An explanation for this discrepancy has recently been given by Söderlind *et al* [25], who invoked orbital polarization in addition to the orbital moment induced by spin-orbit coupling (only the latter was included in our calculations). A smaller magnetic moment can lead to a reduced Kerr rotation. Second, in our calculations we used the experimental lattice constant, but the peak at 4–5 eV is very sensitive to the lattice spacing, and can even disappear for smaller lattice constants [18]. Third, our calculations describe highly ideal crystal structures, whereas the experiments were done on polycrystalline thin films produced by ion beam sputtering, the composition being nominally  $\text{Fe}_{52}\text{Co}_{48}$  [17]. The lifetime parameter in our theory serves to a certain extent to simulate 'sample quality', i.e. it supplies some 'band-width' in which the ideal sample that we model can approach the real sample. In view of this, the agreement of our calculations with the measured spectrum is remarkable.

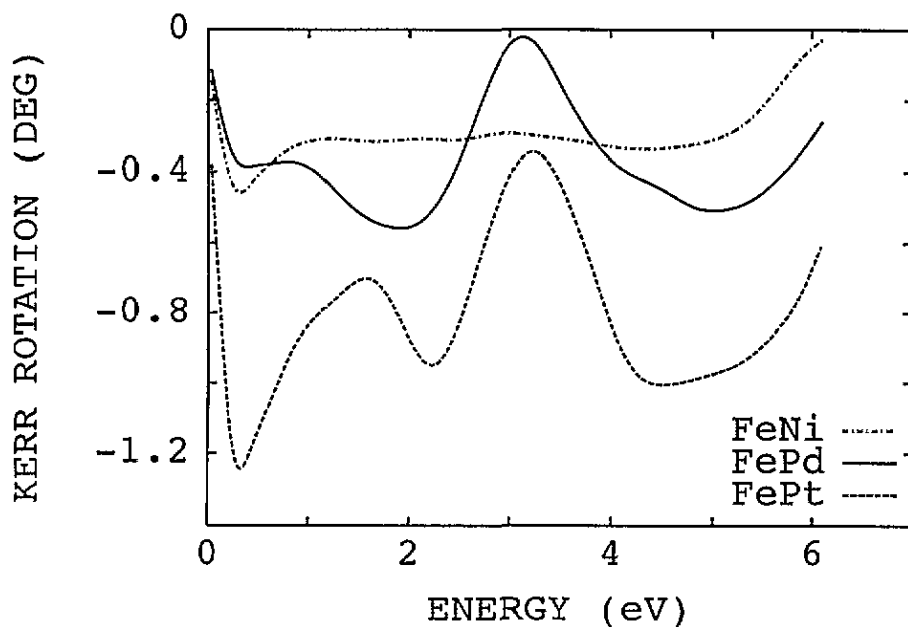


Figure 2. Calculated Kerr spectra for FeNi, FePd and FePt in the CuAu structure. The lifetime parameter used is 0.4 eV for each compound.

### 3.2. FeNi, FePd and FePt

In figure 2 we show the trend in the calculated Kerr spectra of FeNi, FePd and FePt. The increase in the magnitude of the maxima with increasing atomic number is clearly apparent. These calculations were performed for the CuAu structure with a lifetime parameter of 0.4 eV and the experimental lattice constants [26]. By means of numerical experiments in which we changed the spin-orbit coupling parameter locally, we identified the pronounced structure above 4 eV as being due mainly to the Pd and Pt derived electronic states. Since

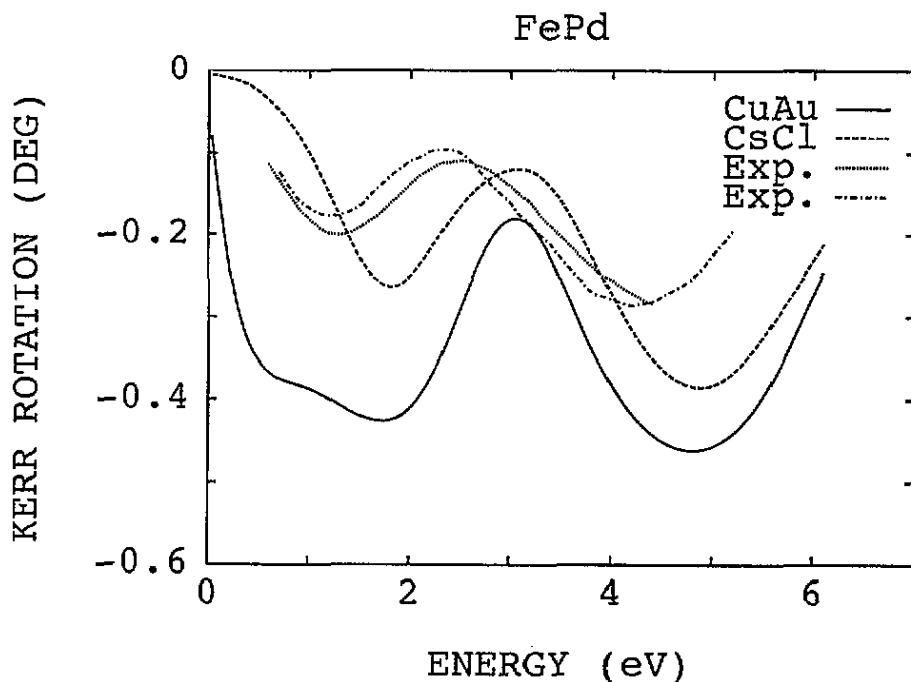


Figure 3. Experimental and theoretical Kerr rotation spectrum of FePd. The experimental results are those of Buschow *et al* [12] (dotted line), and those of Reim *et al* [13] (dashed-dotted line). The full curve is the interband theoretical result for FePd in the CuAu structure, with a lifetime parameter of 0.65 eV; the dashed curve was obtained for the CsCl structure with otherwise the same parameters.

the spin-orbit coupling strength grows with increasing atomic number, it is quite reasonable to assign the trend seen in figure 2 to increasing spin-orbit coupling.

Figure 3 shows the experimental and theoretical Kerr spectra of FePd, the latter having been obtained for the CuAu and the CsCl crystal structures, using experimental atomic volumes and a lifetime parameter of 0.65 eV. The observed crystal structure is CuAu which is also theoretically favoured by its low total energy compared with the CsCl structure. The CuAu lattice constant used was  $a = 3.8598 \text{ \AA}$  and  $c/a = 0.968$  [26]. Also shown in figure 3 are experimental spectra obtained from the work of Buschow *et al* [12] and Reim *et al* [13]. We note that the agreement between theory and experiment is not overwhelming but reasonable, both spectra having a similar two-peak structure, but the theoretical features are more pronounced. Since our calculations give a somewhat larger total average magnetic moment per atom of  $1.69\mu_B$  compared with an experimental value of  $1.6\mu_B$  [26], one might argue that this is the reason for the discrepancy seen in figure 3, in particular since the measurements were made at room temperature where the magnetization is further reduced. The situation is similar, or even worse on first sight, for the case of FePt for which we show our results in figure 4, together with experimental data of Buschow *et al* [12]. (The theoretical FePt spectrum is the same as that of figure 2.) The crystallographic structure used for FePt is the CuAu structure again, with  $a = 3.8609 \text{ \AA}$  and  $c/a = 0.981$  [26]. Again we may compare the total calculated magnetic moments of  $2.918\mu_B$  for Fe and  $0.375\mu_B$  for Pt with experimental values. Neutron diffraction studies point to an Fe moment of  $2.8\mu_B$  at room temperature, but to an average magnetic moment per atom of only  $0.77\mu_B$  [26]. Thus

the moments may be arranged ferrimagnetically. For this, however, we find no theoretical evidence since our calculations predict a stable ferromagnetic alignment.

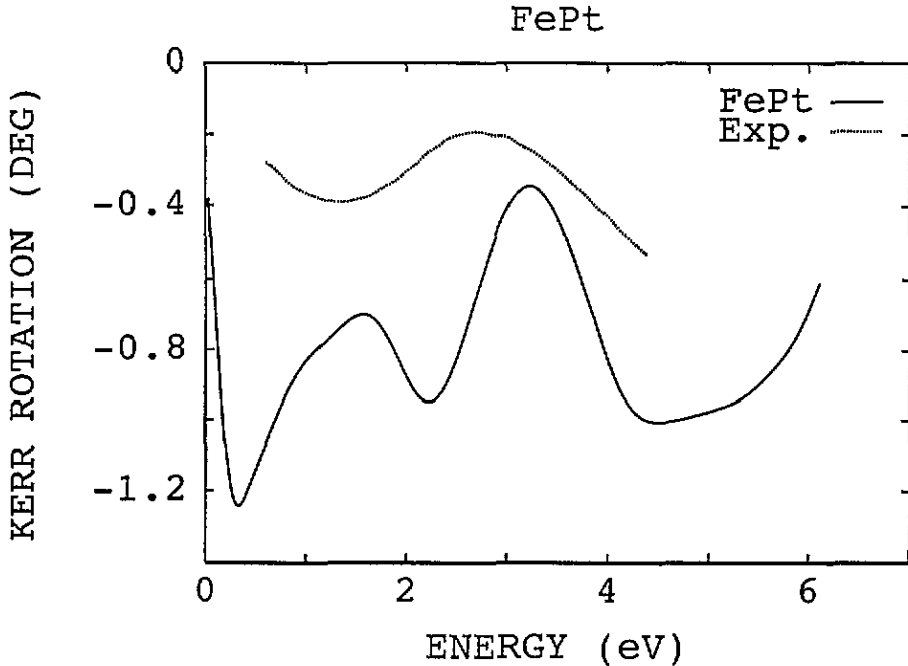


Figure 4. As figure 3, but for FePt. The dotted curve shows the experiment of Buschow *et al* [12]. The full curve gives the calculated interband Kerr rotation of FePt in the CuAu structure, with a lifetime broadening of 0.4 eV.

Just as in the case of FeCo, a more likely explanation for these differences is our use of idealized crystal structures that do not represent the surface and bulk conditions possessed by the samples investigated. This point of view receives further strong support from preliminary measurements [27] on single-crystal FePt, which yield a Kerr spectrum of much larger amplitude than the earlier experimental results shown in figure 4. In the frequency range below 1 eV there is a peak in the theoretical curve that does not appear in the experimental spectra. This difference—as pointed out above—is due to the neglect of the intraband conductivity which strongly affects the Kerr rotation in this energy range [4] and any reasonable choice for the Drude term will remove this peak.

#### 4. Discussion

Turning again to FeCo, figure 1, we may first ask for the physical reason that gives rise to the rather large Kerr angle at about 1.5 eV, because this feature is missing from both Fe and Co, a fact that is nicely demonstrated by Weller *et al* [17]. In view of the rather complicated connection (1) of the Kerr angle with the elements of the conductivity tensor, the latter, especially  $\sigma_{xy}$ , being connected in an involved way with the band structure, it does not make too much sense to search for individual band structure feature to furnish an explanation. Less detailed insight, however, is provided by the observation that Fe is a weak

ferromagnet, (BCC) Co is a strong ferromagnet and so is FeCo, see, e.g., [28]. Thus the Kerr angle benefits from the large magnetization absent in Co and the strong ferromagnetism absent in Fe; responsible in detail are hybrid states that are absent in both Fe and Co but are present in FeCo where they are caused mainly by spin-orbit coupling. The second theoretical peak at 4–5 eV (figure 1) is completely missing from the experimental spectrum, which is surprising, as both (FCC) Fe and (BCC) Co do have small MO peaks at this energy [17]. Previously we showed that for lattice constants about 4% smaller than the optimized theoretical one this peak disappears [18].

Turning now to the MO spectra of FePd and of FePt, figures 2, 3 and 4, we note that they are similar to the CoPd and CoPt spectra [12, 15, 16]: there is a broad maximum in the UV spectral range at about 4–5 eV and a second maximum at about 1.5 eV. The nature of these maxima was previously studied experimentally [13, 16]: within an atomistic picture one can assert that at 4 eV predominantly optical transitions in Pd and Pt are responsible for the shape of the spectra, while in the low-energy range optical transitions dominate in Co or Fe. Our analysis of the trend shown in figure 2 given above and the experimental data show that in these compounds the role of Pd or Pt is mainly to create, through hybridization with states on the 3d atoms, states that contain the stronger spin-orbit interaction of the Pd and Pt states. The effect of Pd and Pt on the electronic structure is nearly identical, apart from the stronger spin-orbit interaction of Pt. Previously Oppeneer *et al.* [5], by means of numerical calculations, established the connection between the spin-orbit coupling strength and the Kerr angle and showed that the latter increases linearly with increasing coupling strength.

Concerning the role of sample preparation, namely disorder and differently ordered crystalline phases, we point out that there are many experimental examples in the literature that show the large influence these facts have, not only on the magnetization [26], but also on the Kerr spectrum. An older, well known example is that of MnBi, which exists in two crystallographic phases, a high-temperature and a low-temperature phase. The Kerr angles of these phases differ by a factor of two [29]. More recently it has been found for TbFe alloys that changes of only a few percent in the Tb concentration can lead to a complete reversal of the Kerr spectrum [30]. Furthermore, in a previous study on Fe [4], it was found that the calculations of the optical conductivity of Fe describe single-crystal data excellently [31], but polycrystalline data rather poorly [32]. Most certainly, there are also important surface effects. These experimental findings and the outcome of our calculations show that there is a strong dependence of the Kerr spectrum on the detailed nature of the atomic environment. For further progress, evidently, more experiments on well defined samples of FePd and FePt are highly desirable.

### Acknowledgments

We gratefully acknowledge partial financial support by the DFG, SFB 252, Darmstadt/Frankfurt/Mainz. We are also grateful to Dr D Weller for informing us of his measurements on FePt.

### References

- [1] Ebert H 1989 *Physica B* **161** 175
- [2] Ebert H and Akai H 1990 *J. Appl. Phys.* **67** 4798
- [3] Halilov S V and Uspenskii Y A 1990 *J. Phys.: Condens. Matter* **2** 6137



- [4] Oppeneer P M, Maurer T, Sticht J and Kübler J 1992 *Phys. Rev. B* **45** 10924
- [5] Oppeneer P M, Sticht J, Maurer T and Kübler J 1992 *Z. Phys. B* **88** 309
- [6] Halilov S V and Feder R 1993 *Int. J. Mod. Phys. B* **7** 683
- [7] Reim W and Schoenes J 1990 *Ferromagnetic Materials* vol 5, ed K H J Buschow and E P Wohlfarth (Amsterdam: North-Holland) p 133
- [8] Schoenes J 1992 *Materials Science and Technology* vol 3, ed R W Cahn, P Haasen and E J Kramer (Weinheim: Chemie) p 147
- [9] Misemer D K 1988 *J. Magn. Magn. Mater.* **72** 267
- [10] Schwarz K 1986 *J. Phys. F: Met. Phys.* **16** L211
- [11] Brändle H, Weller D, Scott J C, Sticht J, Oppeneer P M and Güntherodt G 1993 *Int. J. Mod. Phys. B* **7** 345
- [12] Buschow K H J, van Engen P G and Jongebreur R 1983 *J. Magn. Magn. Mater.* **38** 1
- [13] Reim W, Brändle H, Weller D and Schoenes J 1991 *J. Magn. Magn. Mater.* **93** 220
- [14] Katayama T, Sugimoto T, Suzuki Y, Hashimoto M, de Haan P and Lodder J C 1992 *J. Magn. Magn. Mater.* **104–107** 1002
- [15] Weller D, Brändle H, Gorman G, Lin C-J and Notarys H 1992 *Appl. Phys. Lett.* **61** 2726
- [16] Zeper W B, Greidanus F J A M, Garcia P F and Fincher C R 1989 *J. Appl. Phys.* **65** 4971
- [17] Weller D, Reim W, Ebert H, Johnson D D and Pinski F J 1988 *J. Physique Coll. Suppl.* **12 49 C8** 41
- [18] Oppeneer P M, Sticht J and Herman F 1991 *J. Magn. Soc. Japan* **15** S1 73
- [19] Maurer T, Sticht J, Oppeneer P M, Herman F and Kübler J 1992 *J. Magn. Magn. Mater.* **104–107** 1029
- [20] Williams A R, Kübler J and Gelatt C D 1979 *Phys. Rev. B* **19** 6094
- [21] Andersen O K 1975 *Phys. Rev. B* **12** 3060
- [22] Oppeneer P M unpublished
- [23] *Landolt-Börnstein New Series* 1971 Group III, vol 6 (Berlin: Springer)
- [24] *Landolt-Börnstein New Series* Group III, vol 19a (Berlin: Springer)
- [25] Söderlind P, Johansson B and Eriksson O 1992 *J. Magn. Magn. Mater.* **104–107** 2037
- [26] Villars P and Calvert L D 1985 *Pearson's Handbook of Crystallographic Data for Intermetallic Phases* (Metals Park, OH: American Society for Metals)
- [27] Weller D 1993 private communication
- [28] Schwarz K, Mohn P, Blaha P and Kübler J 1984 *J. Phys. F: Met. Phys.* **14** 2659
- [29] Buschow K H J 1988 *Ferromagnetic Materials* vol 4, ed E P Wohlfarth and K H J Buschow (Amsterdam: North-Holland) p 558
- [30] Krishnan R, Sikora T, Siroky P, Tessier M and Višňovský S Š 1991 *J. Magn. Soc. Japan* **15** S1 79
- [31] Yolken H T and Kruger J 1965 *J. Opt. Soc. Am.* **55** 892
- [32] Johnson P B and Christy R W 1974 *Phys. Rev. B* **9** 5056